



# A robust data processing method for pulse-decay measurement of tight materials

Mingbao Zhang<sup>#</sup>, Yue Wang<sup>#</sup>, Zhiguo Tian, Moran Wang<sup>\*</sup>

Department of Engineering Mechanics, Tsinghua University, Beijing, 100084, China

## ARTICLE INFO

### Keywords:

Porous media  
Permeability  
Pulse decay method  
Data processing  
Leakage

## ABSTRACT

The pulse-decay method is a widely-adopted transient technique for measuring the permeability of tight materials. Given that the gas pressure within the pulse-decay apparatus during the measurement is much higher than atmospheric pressure, gas leakage is usually inevitable, more or less, which may potentially introduce significant errors in the permeability measurements. The data is always discarded and unpublished once a leakage is remarkable. There lacks reasonably explained and conveniently applicable approach for data processing at present. This study proves that the data with slight gas leakage during measurements are still useful and recover the correct value of permeability. To achieve that, a mathematical model accounting for gas leakage is developed and solved. The analytical solution unveils that when gas leakage is present, the logarithm of bilateral pressure difference deviates from a straight line, which depends on the leakage rate and the size of the two chambers. A new data processing method for calculating permeability is proposed by using the unilateral pressure difference over a given time interval. The method corrects the permeability by eliminating the redundant term due to leakage in the analytical solution and is validated by experimental data. The applicability and reliability of pulse decay measurement data will be significantly enhanced.

## 1. Introduction

Tight porous materials are widely used in geological, chemical, and aerospace fields, such as unconventional oil and gas extraction [1,2], carbon dioxide sequestration [3–5], nuclear waste disposal [6–8], and spacecraft lubrication [9–11]. Permeability, a key parameter in the characterization of tight materials, represents the ability of porous media to allow fluids to pass through [12–14]. The pore size of tight porous materials typically measures on the nanoscale, and the permeability ( $<10^{-16} \text{ m}^2$ ) is significantly lower than that of conventional porous media [15,16]. As the permeability of porous media decreases, the time required for laboratory permeability measurements increases, along with an increase in the difficulty of the measurements [17–19].

Laboratory permeability measurement methods can be divided into two categories based on their time characteristics: steady-state methods [20] and unsteady-state methods [21,22]. The latter category includes the pulse-decay method [23], the Gas Research Institute (GRI) method [24,25], and the pressure oscillation method [26,27], among others. Compared with steady-state methods, unsteady-state methods are

generally considered more suitable for measuring the permeability of low-permeability porous media [28–31].

The pulse decay method is one of the most popular transient measurement techniques [32–34], where the core sample is typically connected to chambers with finite volumes at both ends [23,35,36]. After achieving initial equilibrium, some gas is injected into the upstream chamber, thereby creating a pressure higher than that in the downstream chamber. This pressure difference drives the gas to flow from upstream through the sample to downstream, leading to a decrease in upstream pressure and an increase in downstream pressure. Hsieh et al. [37] and Dicker and Smits [38] highlighted that if the applied pulse amplitude is small enough, the pressure difference between both sides of the sample (hereafter referred to as “bilateral pressure difference”) will decay exponentially with time after a sufficiently long period, and this decay rate can be utilized for permeability evaluation [39,40]. Recently the large pressure amplitude scheme has been attempted to be utilized and relevant solutions have been proposed [41–43]. Subsequent researchers have proposed various improved pulse-decay experimental schemes, such as maintaining a constant pressure at one end of the

\* Corresponding author.

E-mail address: [mrwang@tsinghua.edu.cn](mailto:mrwang@tsinghua.edu.cn) (M. Wang).

<sup>#</sup> MZ and YW contribute equally to this work.

sample [29,44-49] or sealing one end [50,51]. There are also many theoretical data processing methods proposed for different effects [35, 52-54]. Compared with the GRI method and the pore pressure oscillation method, the pulse-decay method, with its capability to apply confining pressure simulating the subsurface stress environment and simple experimental setup, is more prevalently used [55].

In most previous studies concerning the pulse-decay method, it was presumed that there was no gas leakage during the measurement, or that the impact of leakage could be disregarded [51,56-59]. However, the experimental setup contains multiple components such as joints and valves [60–62], and the pressure inside the setup is typically much higher than atmospheric pressure. Consequently, gas leakage is inevitable during the general measurement. Besides, as the sample permeability decreases and the measurement time increases, the impact of gas leakage on the pulse decay process may become more significant. Song et al. [63] investigated the measurement uncertainty during pulse decay by setting up an experiment in which the upstream chamber volume was adjusted by opening and closing two valves. They found that the measurements when the valves were not operated to change the volume were closer to the true value, which may be related to the small leakage of the valves. Boulin et al. [64] observed in their experiments that when leakage is present in the upstream chamber, the downstream pressure may eventually exceed the upstream pressure. Heller et al. [65] noted that gas leakage during testing causes the logarithm of the bilateral pressure difference to present as a curve, rather than a straight line, in the late-time stages. Therefore, if gas leakage is ignored and the curve is fitted directly, utilizing the fitted slope value for sample permeability calculation may yield significant errors. Both Boulin et al. [64] and Heller et al. [65] suggested adding a linearly increasing correction term to the pressure data measured in the leaking chamber and using the corrected pressure data for permeability calculation, yet neither provided a rationale for this approach.

According to the above analyses and previous reviews, gas leakage during pulse decay is unavoidable and cannot be ignored. Meanwhile, there is no reasonable and easy-to-use correction method so far. In light of the aforementioned issues and objectives, this work is organized into the following sections: In Section 2, the governing equation and boundary conditions in the presence of leakage are provided. A new method of data processing and correction is proposed based on the analytical solution. In addition, the effects of different upstream and downstream volumes and leakage rates on the pressure profile are analyzed. In Section 3, the proposed correction method is validated using experimental data from the literature. Finally, conclusions are presented in Section 4. This work holds significant importance for data

processing of various pulse-decay experimental schemes in low permeability porous media.

## 2. Mathematical and physical model

Combined with the physical process of pulse decay method, a reasonable mathematical model can be obtained. After rigorous solving, new data processing methods can be considered from the perspective of analytical solutions. In this section, the mathematical and physical model of the pulse decay process in the presence of leakage will be carried out from the fundamental governing equations. The analytical solution obtained will guide the new data processing method and the analysis of the effects due to gas leakage.

### 2.1. Governing equation and analytical solution

In the original pulse-decay method proposed by Brace et al. [23], a cylindrical porous media sample is situated in a holder, with chambers of finite volume connected at both ends of the sample, as depicted in Fig. 1. Given that the lateral side of the sample in the experiment is typically enclosed in foil or casing and is compacted by a confining pressure pump [33], it can be assumed that there is no leakage on the lateral side. Consequently, gas leakage only takes place at both ends of the sample, specifically within the upstream and downstream chambers. When the initial pressure difference between the upstream and downstream is adequately small, Brace et al. combining Darcy’s law with the law of mass conservation, derived the governing equation for the pulse-decay process in a homogeneous sample as follows [12,66,67]:

$$\frac{\partial P}{\partial t} = \frac{k}{\beta_p \mu \phi} \frac{\partial^2 P}{\partial x^2}, \quad (1)$$

where  $P$  [Pa] is the pore pressure,  $k$  [ $\text{m}^2$ ] is the permeability coefficient,  $\beta_p$  [ $\text{Pa}^{-1}$ ] is the fluid compressibility,  $\mu$  [ $\text{Pa}\cdot\text{s}$ ] is the dynamics viscosity of the fluid,  $\phi$  is the sample porosity,  $x$  [m] and  $t$  [s] are the spatial and temporal coordinates, respectively.

According to the law of mass conservation, the reduction in gas mass within the upstream chamber should equate to the sum of the mass flow rate into the sample and the leakage from the upstream chamber:

$$\left. \frac{\partial(\rho V_u)}{\partial t} \right|_{x=0} = \rho \left. \frac{kA}{\mu} \frac{\partial P}{\partial x} \right|_{x=0} - \rho Q_u, \quad (2)$$

where  $\rho$  [ $\text{kg}\cdot\text{m}^{-3}$ ] is the density of the fluid,  $V_u$  [ $\text{m}^3$ ] is the volume of

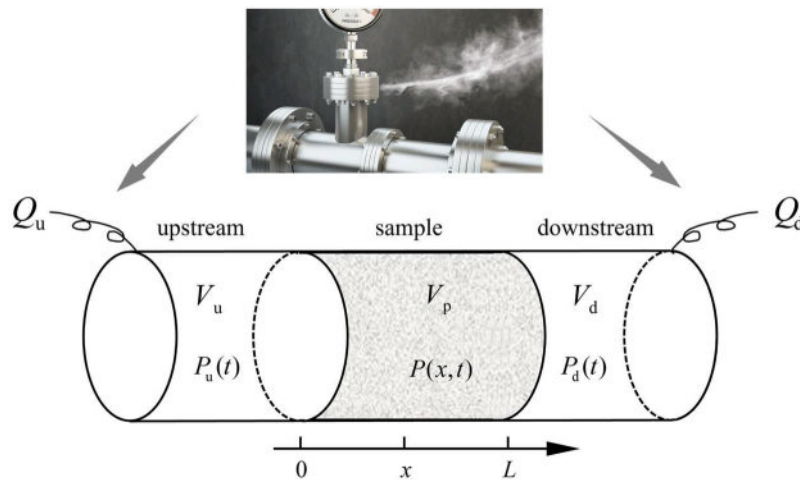


Fig. 1. The scheme of the standard two-chamber pulse-decay test.  $Q_u$  and  $Q_d$  indicate that there may be leakage in the chambers on both sides.  $V_u$ ,  $V_d$ ,  $V_p$  represent the upstream chamber, downstream chamber and porous sample volume, respectively. The spatial coordinates are 0 at the upstream and sample boundary and  $L$  at the sample and downstream boundary.

the upstream,  $A$  [m<sup>2</sup>] is the sample's cross-sectional area,  $Q_u$  [m<sup>3</sup>•s<sup>-1</sup>] is the upstream leakage flow rate. By rewriting the above equation in terms of pressure  $P$  as the independent variable, the expression for the upstream boundary condition can be obtained as follows:

$$\left. \frac{\partial P}{\partial t} \right|_{x=0} = \frac{k}{\beta_p \mu} \frac{A}{V_u} \left. \frac{\partial P}{\partial x} \right|_{x=0} - \frac{Q_u}{V_u \beta_p} \quad (3)$$

Similarly, the downstream boundary condition can be derived as follows:

$$\left. \frac{\partial P}{\partial t} \right|_{x=L} = -\frac{k}{\beta_p \mu} \frac{A}{V_d} \left. \frac{\partial P}{\partial x} \right|_{x=L} - \frac{Q_d}{V_d \beta_p} \quad (4)$$

Here,  $L$  [m] is the length of the cylindrical sample,  $V_d$  [m<sup>3</sup>] is the volume of the downstream,  $Q_d$  is the downstream leakage flow rate. Given that leakage in the pulse-decay experimental setup typically occurs at valves or joints, it falls within the category of small-hole leakage [68]. Both theoretical analyses and experimental results suggest that at this juncture, the leakage rates  $Q_u$  and  $Q_d$  can be approximated as constants [65,68,69]. The assumption of constant leakage rate holds to a significant extent when the pressure is far greater than the ambient pressure, primarily due to the occurrence of subsonic choking [70,71]. When both upstream and downstream leakage rates are zero, Eqs. (3) and (4) reduce to the typical boundary conditions for the pulse-decay process as outlined in the literature. The initial conditions of the pulse-decay process depend on the way the initial pulse is applied. Without loss of generality, here the initial pulse is assumed to be applied by pressurizing the upstream side:

$$P(x, 0) = \begin{cases} P_u(0), & x = 0 \\ P_d(0), & 0 < x \leq L \end{cases} \quad (5)$$

where  $P_u(0)$  [Pa] and  $P_d(0)$  [Pa] represent the pressures within the upstream and downstream chambers at the moment the pulse is applied, respectively.

To facilitate analysis and solution, it is necessary to introduce the following non-dimensional variables:

$$P_D(t) = \frac{P(t) - P_d(0)}{P_u(0) - P_d(0)}, \quad t_D = \frac{kt}{\beta_p \mu \phi L^2}, \quad x_D = \frac{x}{L}, \quad V_{uD} = \frac{LA\phi}{V_u}, \quad V_{dD} = \frac{LA\phi}{V_d} \quad (6)$$

where  $V_{uD}$  and  $V_{dD}$  are the ratios of the pore volume to the upstream and downstream volume, respectively. Combing the above dimensionless parameters, the non-dimensional form of the governing equation, and the boundary and initial conditions can be obtained as follows:

$$\frac{\partial P_D}{\partial t_D} = \frac{\partial^2 P_D}{\partial x_D^2} \quad (7)$$

$$\left. \frac{\partial P_D}{\partial t_D} \right|_{x_D=0} = V_{uD} \left. \frac{\partial P_D}{\partial x_D} \right|_{x_D=0} - V_{uD} Q_{uD}, \quad (8)$$

$$\left. \frac{\partial P_D}{\partial t_D} \right|_{x_D=1} = -V_{dD} \left. \frac{\partial P_D}{\partial x_D} \right|_{x_D=1} - V_{dD} Q_{dD}, \quad (9)$$

$$P_D(x_D, 0) = \begin{cases} 1, & x_D = 0 \\ 0, & 0 < x_D \leq 1 \end{cases} \quad (10)$$

Here, the non-dimensional upstream and downstream leakage rates,  $Q_{uD}$  and  $Q_{dD}$ , are defined as follows:

$$Q_{uD} = \frac{Q_u \mu L}{kA[P_u(0) - P_d(0)]}, \quad Q_{dD} = \frac{Q_d \mu L}{kA[P_u(0) - P_d(0)]} \quad (11)$$

Eqs. (7)–(10) constitute the boundary value problem for the pulse-decay process in the presence of gas leakage. Compared to the scenario without leakage, the emergence of gas leakage introduces inhomogeneous terms, proportional to the leakage rate, into the boundary

conditions of the pulse-decay process. It should be noted that these inhomogeneous terms also depend on the ratio of the pore volume of the sample to the volumes of the upstream and downstream chambers.

This boundary value problem can be addressed by dividing the solution into two parts: the first part being a particular solution that complies with the inhomogeneous boundary conditions, and the second part being the general solution satisfying the homogeneous boundary conditions. By combining these two components, an expression for the pressure distribution within the sample, in the presence of gas leakage, can be derived:

$$P_D(x_D, t_D) = Mt_D + \frac{M}{2}x_D^2 + Nx_D + C_0 + \sum_{m=1}^{\infty} C_m X_m(x_D) \exp(-\theta_m^2 t_D), \quad (12)$$

where  $C_m$  ( $m \geq 1$ ) is a constant coefficient related to the specific initial conditions,  $X_m$  is the eigenfunction corresponding to the homogeneous boundary conditions,  $\theta_m$  is the  $m$ th positive root of the transcendental Eq. (13), and the expressions for  $M$  and  $N$  are as shown in Eq. (14):

$$\tan \theta = \frac{(V_{uD} + V_{dD})\theta}{\theta^2 - V_{uD}V_{dD}}, \quad (13)$$

$$M = -\frac{V_{uD}V_{dD}Q_{uD} + V_{dD}Q_{dD}}{V_{dD} + V_{uD} + V_{dD}}, \quad N = \frac{(V_{uD} + V_{dD})Q_{uD} - V_{dD}Q_{dD}}{V_{dD} + V_{uD} + V_{dD}} \quad (14)$$

The detailed solution process can be found in the appendix.

The upstream and downstream pressures can be deduced by setting  $x_D = 0$  and  $x_D = 1$  in Eq. (12), respectively. Upon analysis, it is evident that in the absence of leakage, both  $M$  and  $N$  equate to zero, and the upstream and downstream pressures are composed of only a constant term and a series of exponential function terms. Conversely, when gas leakage is present, an additional term manifesting a linear decay with time appears in both the upstream and downstream pressures. The first two terms in Eq. (12) offer a theoretical basis for the suggestion made by Boulin et al. [64] to introduce linear correction terms to the upstream and downstream pressure data in the presence of gas leakage. Furthermore, it is determined that, while the correction terms for upstream and downstream should increase at the same rate, they should differ by a constant value.

After a sufficiently long duration from the beginning of the experiment, in the absence of leakage, the pressure at each point in the sample will converge to the equilibrium pressure. Nevertheless, in the presence of leakage, Eq. (12) reveals that the pressure distribution within the sample can be expressed as:

$$P_D(x_D, t_D) \approx Mt_D + \frac{M}{2}x_D^2 + Nx_D + C_0, \quad (t_D \gg 1) \quad (15)$$

This indicates that the typical concept of equilibrium pressure may no longer be applicable when leakage occurs. In such circumstances, the pressure at each position within the sample will continue to decrease over time, and after a sufficiently long period, a stable pressure gradient will be maintained within the sample, which suggests the continued existence of directional gas flow within the sample at this stage.

When one side of the sample is connected to a gas pump to maintain constant pressure, it can be construed that this side is connected to a chamber with an "infinitely large" volume. In this case, the ratio of the sample's pore volume to the volume of that side's chamber becomes zero. Substituting  $V_{uD} = 0$  or  $V_{dD} = 0$  into Eq. (12) yields:

$$P_D(x_D, t_D) = -Q_{dD}x_D + C_0 + \sum_{m=1}^{\infty} C_m X_m(x_D) \exp(-\theta_m^2 t_D), \quad (V_{uD} = 0) \quad (16)$$

$$P_D(x_D, t_D) = Q_{uD}x_D + C_0 + \sum_{m=1}^{\infty} C_m X_m(x_D) \exp(-\theta_m^2 t_D), \quad (V_{dD} = 0) \quad (17)$$

It should be noted that although there may be a leakage in the upstream chamber, only the downstream leakage flow rate,  $Q_{dD}$ , is reflected in Eq. (16). Since a gas pump continuously feeds gas into the

upstream chamber, the upstream pressure maintains a constant. Consequently, changing the upstream leakage rate affects only the power of the gas pump and not the value of the upstream pressure. When the downstream pressure remains constant, a similar conclusion can be drawn from Eq. (17). Furthermore, in contrast to the scenario where the volumes of the chambers at both ends are finite, there is no more than a linear decay term over time in the system. Hence, the linear correction method is ineffective for processing leakage data when the pressure is constant on one side. From Eqs. (16) and (17), it can be inferred that after a sufficient amount of time, the system can reach a steady state in which the pressure within the system shows a linear distribution from upstream to downstream.

## 2.2. Data processing and correction method

Brace et al. [23] and Dicker and Smits [38] analyzed the pulse-decay process in the absence of leakage and found that by taking the logarithm of the bilateral pressure difference, a straight line is obtained during the late-time stage of the experiment. The slope of this line correlates with the permeability of the sample. However, in the presence of gas leakage, the expression for the bilateral pressure difference, derived from Eq. (12), is as follows:

$$\Delta P_D(t_D) = -\frac{M}{2} - N + \sum_{m=1}^{\infty} C_m [X_m(0) - X(1)] \exp(-\theta_m^2 t_D). \quad (18)$$

This shows that when gas leakage is present, the bilateral pressure difference,  $\Delta P_D$ , consists of not only exponential terms but also a constant term. Consequently, the direct application of the logarithm to the  $\Delta P_D$  will result in a curve, rather than a straight line, in the late-time stage.

The detailed expression for the constant term is:

$$\frac{M}{2} - N = \frac{(V_{uD} V_{dD} + 2V_{dD}) Q_{dD} - (V_{uD} V_{dD} + 2V_{uD}) Q_{uD}}{2(V_{uD} V_{dD} + V_{uD} + V_{dD})}. \quad (19)$$

This reveals that the value of the constant term is dependent on the volume ratio  $V_{uD}, V_{dD}$  and the leakage rates at both ends  $Q_{uD}, Q_{dD}$ . Therefore, the constant term in Eq. (18) invalidates the logarithmic bilateral pressure difference approach. Several researchers proposed the introduction of time-increasing linear correction terms to adjust the pressure data in the leakage chamber, and then use the corrected pressure data for permeability calculation [64,65]. However, it often requires multiple trials in practice to determine the best-fit values of the correction terms, making the process inconvenient.

In the authors' previous publication [40], it was highlighted that in addition to the commonly used bilateral pressure difference, the "unilateral pressure change" can also be utilized for permeability calculation in pulse-decay measurements without leakage. As illustrated in Fig. 2, the unilateral pressure difference,  $\Delta_{\tau} P_{uD}$  or  $\Delta_{\tau} P_{dD}$ , refers to the absolute value of the pressure change on the upstream or downstream side of the sample within a specified time interval,  $\Delta\tau$ . According to Eq. (12), the late-time expression for the upstream and downstream unilateral pressure difference in case of gas leakage is:

$$\Delta_{\tau} P_{uD}(t_D) \approx -M\Delta\tau + C_1 X_1(0) [1 - \exp(-\theta_1^2 \Delta\tau)] \exp(-\theta_1^2 t_D), \quad (20)$$

$$\Delta_{\tau} P_{dD}(t_D) \approx M\Delta\tau + C_1 X_1(1) [\exp(-\theta_1^2 \Delta\tau) - 1] \exp(-\theta_1^2 t_D), \quad (21)$$

where the symbol " $\approx$ " indicates that the equality holds mainly in the late-time stage. It can be observed that when gas leakage is present, the unilateral pressure difference also contains a constant term in addition to the exponential term. However, as the constant terms in Eqs. (20) and (21) are opposites, their sum cancels out the constant term:

$$\Delta_{\tau} P_{uD}(t_D) + \Delta_{\tau} P_{dD}(t_D) \approx C_1 [X_1(0) - X(1)] [1 - \exp(-\theta_1^2 \Delta\tau)] \exp(-\theta_1^2 t_D). \quad (22)$$

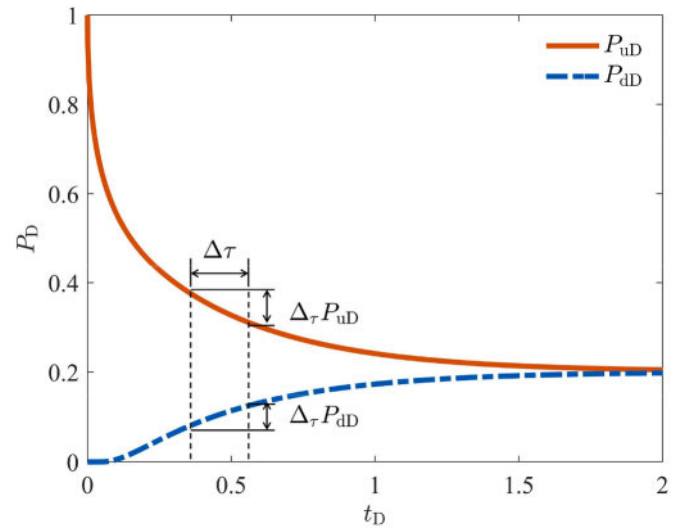


Fig. 2. The scheme of the dimensionless unilateral upstream pressure difference  $\Delta_{\tau} P_{uD}$  and the dimensionless unilateral downstream pressure difference  $\Delta_{\tau} P_{dD}$ . The pressure difference at a specified time interval  $\tau$  is defined as the unilateral pressure difference.

As illustrated in Fig. 2,  $\Delta_{\tau} P_{uD}(t_D) + \Delta_{\tau} P_{dD}(t_D)$  represents the sum of the unilateral pressure difference in upstream and downstream pressures over the time interval  $\Delta\tau$ . Since the late-time expression of  $\Delta_{\tau} P_{uD}(t_D) + \Delta_{\tau} P_{dD}(t_D)$  contains only a single exponential term, its logarithm will yield a straight line in the late-time stage.

Taking the logarithm of Eq. (22) and converting the time to a dimensional form yields:

$$\ln[\Delta_{\tau} P_{uD}(t_D) + \Delta_{\tau} P_{dD}(t_D)] \approx f + \alpha t, \quad (23)$$

where  $f$  and  $\alpha$  represent the y-intercept and slope of the late-stage linear section, respectively:

$$f = \ln\{C_1 [X_1(0) - X(1)] [1 - \exp(-\theta_1^2 \Delta\tau)]\}, \quad (24)$$

$$\alpha = -\frac{\theta_1^2 k}{\beta_{\rho} \mu \phi L^2}. \quad (25)$$

By transforming the expression for the slope  $\alpha$ , an expression for the sample permeability can be derived:

$$k = \frac{\beta_{\rho} \mu \phi L^2}{\theta_1^2}. \quad (26)$$

This suggests that in the presence of gas leakage during the pulse-decay process, the sum of the unilateral upstream and downstream pressure difference within a given time interval can be used to calculate the permeability of the sample.

Specifically, in the case where the upstream pressure is maintained constant ( $V_{uD} = 0$ ), the unilateral upstream pressure change  $\Delta_{\tau} P_{uD}$  will be zero. In such a scenario, the sum of the unilateral upstream and downstream pressure difference,  $\Delta_{\tau} P_{uD} + \Delta_{\tau} P_{dD}$ , will be equivalent to the unilateral downstream pressure difference  $\Delta_{\tau} P_{dD}$ . Likewise, when the downstream pressure is kept constant ( $V_{dD} = 0$ ),  $\Delta_{\tau} P_{uD} + \Delta_{\tau} P_{dD}$  will reduce to  $\Delta_{\tau} P_{uD}$ .

Contrasting with the method that adds correction terms, the application of the sum of the unilateral upstream and downstream pressure difference simplifies the process and eliminates the need for multiple trials. It is notable that Eq. (22) also remains valid in the absence of leakage. In addition, the correction method is also applicable in principle if a liquid is utilized as the measuring medium and the data deviates due to leakage.

### 2.3. Influence of leakage on pressure curve

The theoretical analysis of the pulse decay process with gas leakage is carried out based on the analytical solution obtained above. Firstly, without loss of generality, the influence of leakage on the pulse-decay process is analyzed when the upstream and downstream chamber volumes are equal, and the results are depicted in Fig. 3. Fig. 3(a) display the upstream and downstream pressure curves over time, when there is only upstream leakage ( $Q_{uD} \geq 0, Q_{dD} = 0$ ). Upon comparison to the case with no leakage, the upstream leakage leads to a drop in upstream and downstream pressure, and the drop is proportional to time and the leakage rate. The upstream pressure reduction surpasses the downstream one, leading to the downstream pressure exceeding the upstream pressure after a sufficiently long duration, which is consistent with the experimental observations made by Boulin et al. [64]. Fig. 3(b) consider the case where only the downstream chamber experiences leakage ( $Q_{uD} = 0, Q_{dD} \geq 0$ ). Both the upstream and downstream pressure also show a decrease compared to the no-leakage case, but the decrease in downstream pressure exceeds the decrease in upstream pressure. As a result, the upstream and downstream pressure difference remains stable and positive after a sufficiently long duration. Fig. 3(c) consider the situation where both the upstream and downstream have leakages of equal magnitude ( $Q_{uD} = Q_{dD} \geq 0$ ). Compared to the no-leakage scenario, gas leakage leads to an equivalent decrease in the upstream and downstream pressures. The upstream and downstream pressures eventually converge to be equal. If there is leakage both upstream and downstream and the leakage rates are not equal ( $Q_{uD} \neq Q_{dD} \geq 0$ ), the pressure curve will decrease compared to the case without leaks. However, the relative magnitude of the upstream and downstream pressures ultimately depends on the relative magnitudes of the leak rates, as shown in Fig. 3(d). This is equivalent to the superposition of equal leak rates and unilateral

leaks (Fig. 3(c) superimposed on Fig. 3(a) or Fig. 3(b)).

Gas leakage has caused the deviation of the bilateral logarithmic pressure difference from a straight line as shown in the Fig. 4. If there is only upstream leakage, according to Eq. (19), the term  $-M/2 - N$  would assume a negative value. Consequently, the logarithm of the bilateral pressure difference yields an upward concave curve as shown in the Fig. 4(a). Conversely, if there is only a leak downstream, taking the logarithm of the pressure on both sides will produce a concave curve, as shown in the Fig. 4(b). The degree of concavity is related to the magnitude of the downstream leakage rate. According to Eq. (19), due to the equal volumes of the upstream and downstream chambers and equivalent leakages, the impact of leakage on the upstream and downstream pressure cancels each other out when calculating the bilateral pressure difference. Therefore, a straight line can still be achieved in the late-time stage after taking the logarithm of the bilateral pressure difference as shown in Fig. 4(c). However, ensuring equal upstream and downstream leakage rates in practical measurements is exceedingly challenging. When the leak rates are not equal, the concave or convex orientation of the logarithmic bilateral pressure difference curve depends on the relative magnitudes of the leak rates, as shown in Fig. 4(d).

Subsequently, based on the Eqs. (18) and (20-22), the bilateral pressure difference  $\Delta P_D$ , the unilateral upstream pressure difference  $\Delta \tau P_{uD}$ , the unilateral downstream pressure difference  $\Delta \tau P_{dD}$ , as well as the sum of the unilateral upstream and downstream pressure difference  $\Delta \tau P_{uD} + \Delta \tau P_{dD}$  under the condition of leakage can be obtained as shown in Fig. 5. It is evident that irrespective of the leakage rate variations, the logarithm of  $\Delta \tau P_{uD} + \Delta \tau P_{dD}$  yields a straight line in the late-time stage, while logarithms of the other quantities yield curves.

Furthermore, the impacts of leakage on the pulse-decay process are analyzed when the pressure on one side remains constant, as depicted in Fig. 6. Fig. 6(a) illustrates the pressure curves in upstream and

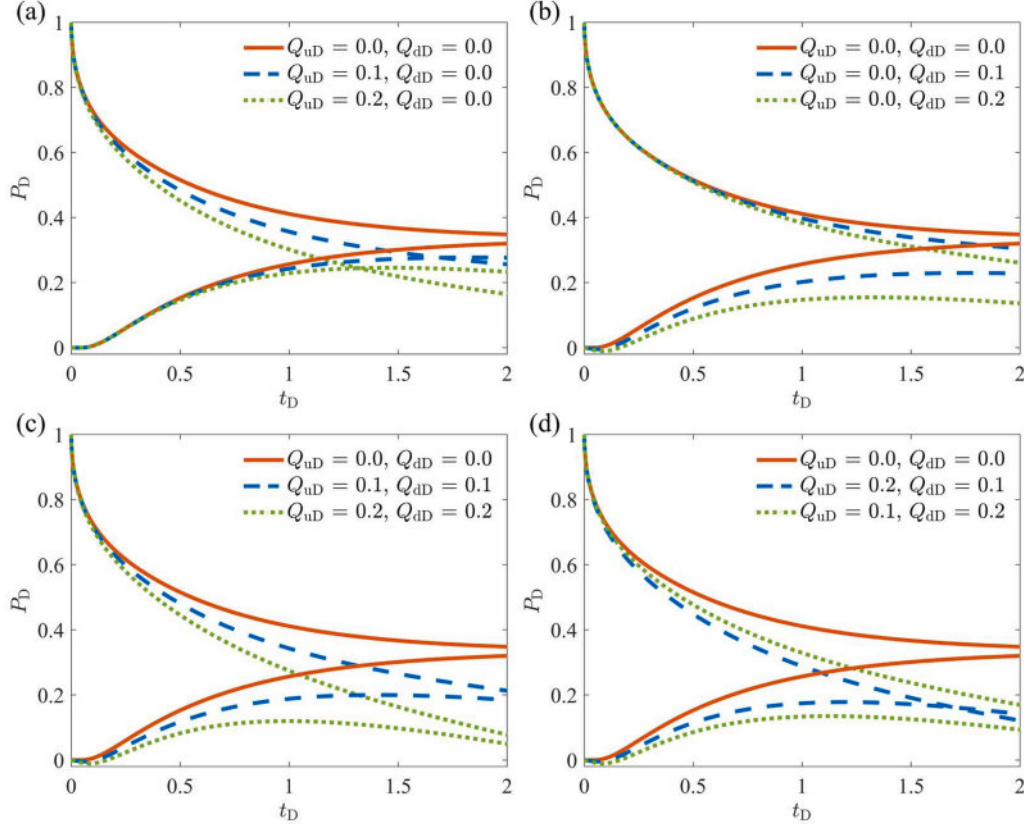


**Fig. 3.** The impact of gas leakage on the upstream and downstream pressure curves when the volumes of the two chambers are equal ( $V_{uD} = V_{dD} = 1$ ). (a) Leakage exists only upstream ( $Q_{uD} \geq 0, Q_{dD} = 0$ ); (b) Leakage exists only downstream ( $Q_{uD} = 0, Q_{dD} \geq 0$ ); (c) Leakage exists both upstream and downstream, and the leakage rates are equal ( $Q_{uD} = Q_{dD} \geq 0$ ); (d) Leakage exists both upstream and downstream, and the leakage rates are not equal ( $Q_{uD} \neq Q_{dD} \geq 0$ ).

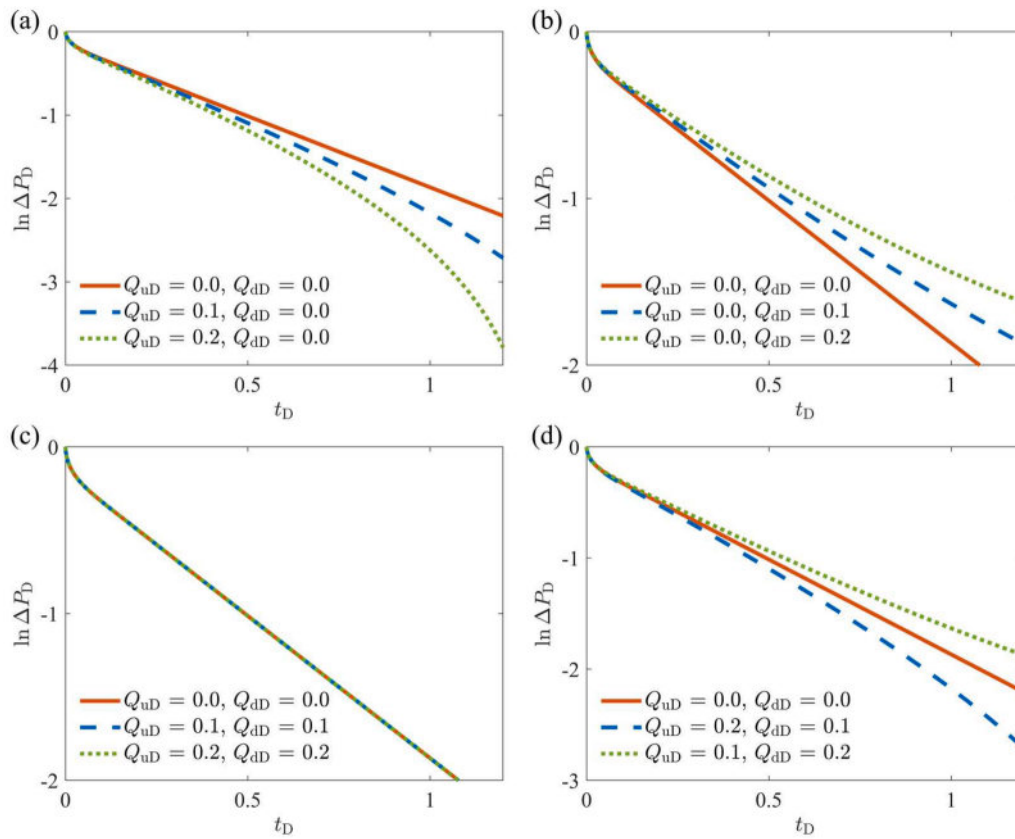


**Fig. 4.** The impact of gas leakage on the logarithmic bilateral pressure difference when the volumes of the two chambers are equal ( $V_{uD} = V_{dD} = 1$ ). (a) Leakage exists only upstream ( $Q_{uD} \geq 0, Q_{dD} = 0$ ); (b) Leakage exists only downstream ( $Q_{uD} = 0, Q_{dD} \geq 0$ ); (c) Leakage exists both upstream and downstream, and the leakage rates are equal ( $Q_{uD} = Q_{dD} \geq 0$ ); (d) Leakage exists both upstream and downstream, and the leakage rates are not equal ( $Q_{uD} \neq Q_{dD} \geq 0$ ).

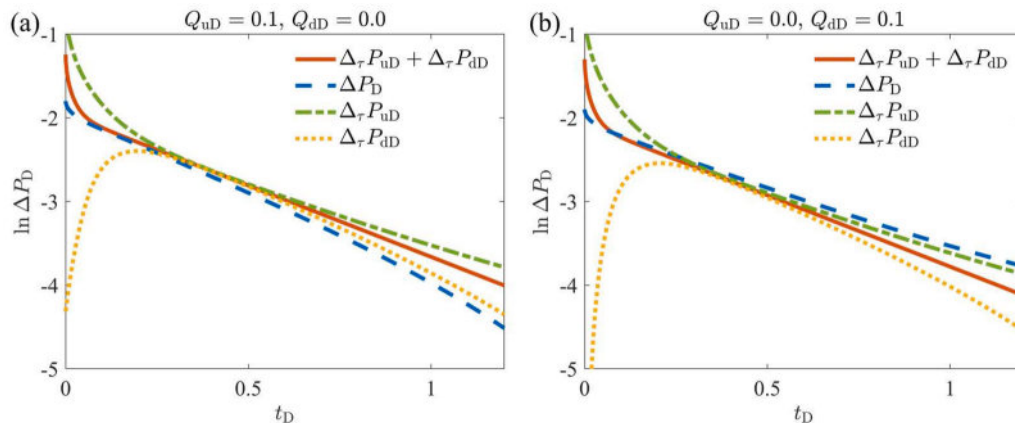


**Fig. 5.** Logarithm curves of the bilateral pressure difference  $\Delta P_D$ , the unilateral upstream pressure difference  $\Delta \tau P_{uD}$ , the unilateral downstream pressure difference  $\Delta \tau P_{dD}$ , and the sum of the unilateral upstream and downstream pressure difference  $\Delta \tau P_{uD} + \Delta \tau P_{dD}$  versus time, when there is leakage ( $V_{uD} = V_{dD} = 1$ ). Only the logarithm of  $\Delta \tau P_{uD} + \Delta \tau P_{dD}$  yields a straight line in the late-time stage.

downstream when the upstream pressure is held constant with different gas leakage rates. In the initial stages of the experiment, the bilateral pressure difference results in a gas flow from the upstream to the downstream, surpassing the downstream leakage and thereby leading to a continuous increase in the downstream pressure. When the pressure-driven flow is equal to the leakage flow, the downstream pressure is stabilized. The magnitude of the eventual bilateral pressure difference depends on the magnitude of the leakage. The downstream volume ratio  $V_{dD}$ , only influences the rate of pressure increase in the downstream but does not alter the magnitude of the eventual bilateral pressure difference

as shown in Fig. 6(b).

Fig. 6(c) demonstrates the pressure curve under the condition of constant downstream pressure with different gas leakage rates. In the initial stage of the experiment, the upstream test gas continued to flow into downstream and leaked to the outside, causing the upstream pressure to drop. After the upstream pressure drops to equal the downstream pressure, because of the presence of leaks and the upstream pressure remains greater than the ambient pressure, the upstream pressure continues to drop, and the gas flows backward from downstream to upstream. When the gas flow from the downstream to the upstream equates

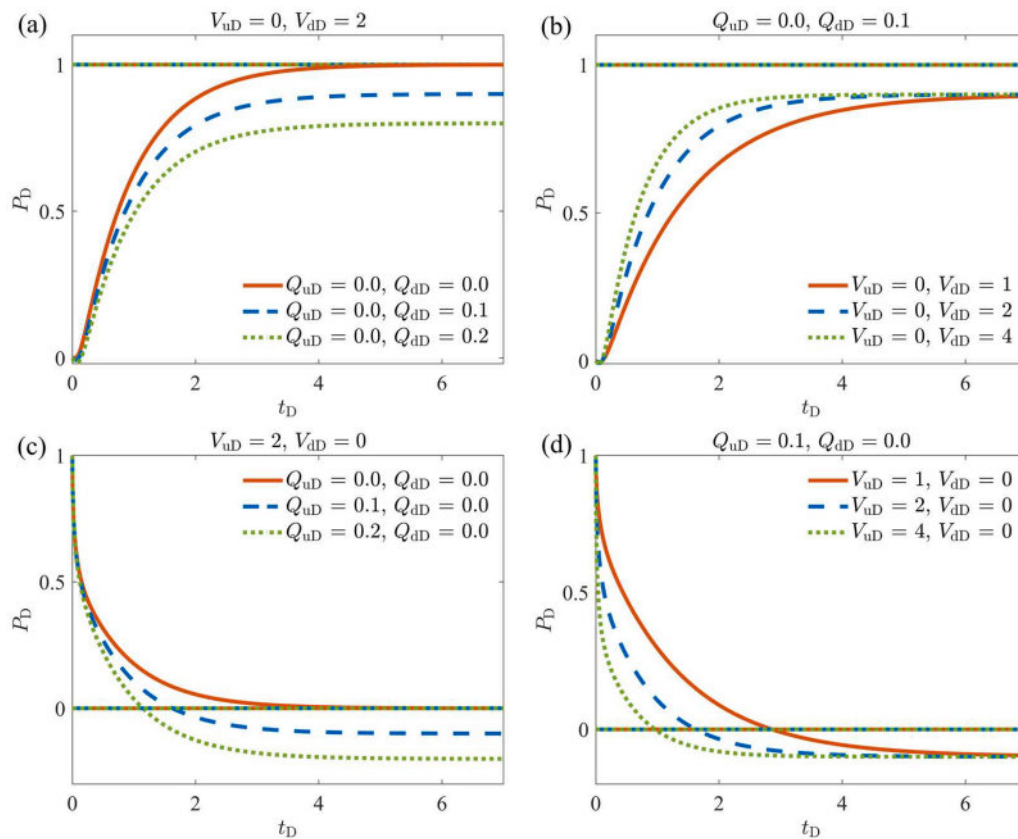


**Fig. 6.** The pressure curve when pressure is kept constant on one side. (a)  $V_{uD} = 0$ : Upstream pressure is maintained constant with different leakage rates; (b)  $V_{uD} = 0$ : Upstream pressure is maintained constant with different volume ratios; (c)  $V_{dD} = 0$ : Downstream pressure is maintained constant with different leakage rates; (d)  $V_{dD} = 0$ : Downstream pressure is maintained constant with different volume ratios.

to the gas leakage from the upstream, the system achieves a steady state. The eventual pressure difference between the upstream and downstream is proportional to the magnitude of leakage and independent of the upstream volume ratio  $V_{uD}$  as shown in Fig. 6(d).

Fig. 7(a) and (b) present the change of the logarithmic unilateral downstream pressure difference,  $\ln \Delta_{\tau} P_{dD}$ , when the upstream pressure is maintained constant. The results show that taking the logarithm of the unilateral downstream pressure creates a straight line in the late-time stage. The magnitude of the leak rate does not affect the slope of the straight line, as shown in Fig. 7(a), indicating that the correction method proposed in this study has eliminated the influence of leaks. The downstream volume ratio  $V_{dD}$  affects the slope and intercept because it appears in the expression for parameter  $\theta$ . Similarly, Fig. 7(c) and (d) illustrate that when the downstream pressure is kept constant, the change in unilateral upstream pressure  $\Delta_{\tau} P_{uD}$  can be utilized for permeability calculations. The upstream volume ratio  $V_{uD}$  affects the slope and intercept of the straight line in the late-time stage.

### 3. Experimental validation

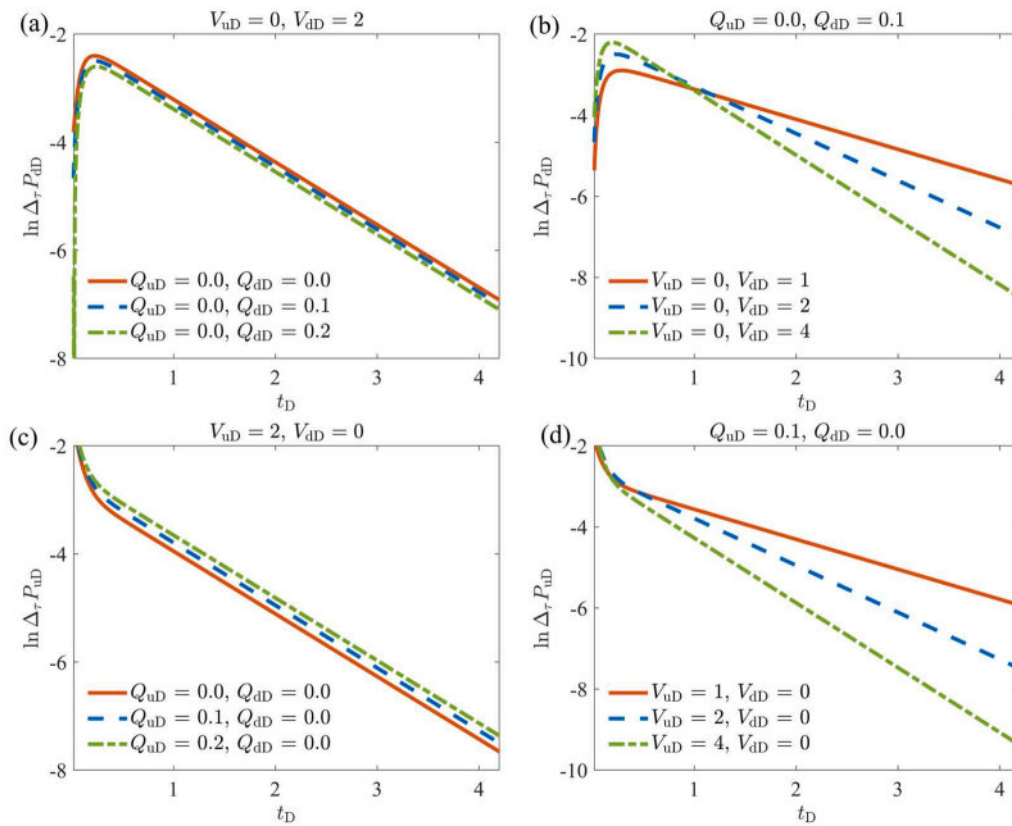
The method proposed above for processing data in the presence of leakage needs to be validated by experimental data. However, in all permeability measurement experiments, gas leakage is avoided as much as possible. Deliberately creating leakage in experiments is uncontrollable and unreasonable. When presenting experimental data, most researchers assert that there is either no gas leakage, or that its impact can be ignored. Data exhibiting significant gas leakage might be considered unusable and consequently discarded. Therefore, the amount of data available for validate the methodology data is minimal.

This section employs experimental data reported by Heller et al. [65] to validate the proposed data processing method. The samples tested by

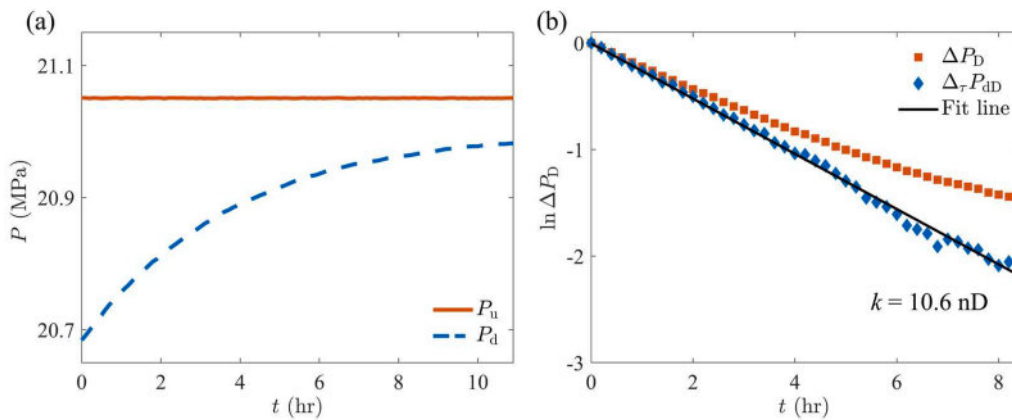
Heller et al. were sourced from Eagle Ford Shale in the United States, and a gas pump was utilized to maintain a constant upstream pressure throughout the experiment. The author kept the number of pipe fittings and valves to the minimum and used relatively small downstream volumes to reduce the impact of leakage. However, the pressure curves in the experimental results still showed the existence of leakage. For a comprehensive introduction to the experimental setup, the tested samples, and the measurement procedures, readers are suggested to refer to the original publication by Heller et al. [65].

Fig. 8(a) illustrates the pressure curves of upstream and downstream in the presence of leakage. The experimental pressure trend is consistent with Fig. 6(a) analyzed above, as the downstream pressure cannot reach the upstream pressure due to the presence of gas leakage and there is always a pressure difference between the two sides. At this pressure difference, the gas flow from upstream to downstream is equal to the downstream leakage rate.

Fig. 8(b) illustrates that due to gas leakage, the direct logarithmic application to the bilateral pressure difference  $\Delta P_D$  results in an upward concave curve, which is consistent with the theoretical prediction of Eq. (18). Based on the proposed method in the previous section, because the upstream pressure remains constant, the sum of the unilateral upstream and unilateral downstream pressure difference,  $\Delta_{\tau} P_{uD} + \Delta_{\tau} P_{dD}$ , will be equivalent to the unilateral downstream pressure difference  $\Delta_{\tau} P_{dD}$ . The downstream pressure data are substituted into Eq. (21) to calculate the unilateral downstream pressure difference  $\Delta_{\tau} P_{dD}$ , which generates a straight line at the late-time stage, thus validating the above theoretical results. Through the fitting of the logarithm of the unilateral downstream pressure difference in the late-time stage, the slope can be obtained by Eq. (23). The apparent permeability of the sample is determined to be 10.6 nD according to Eq. (26). Heller et al. used early-time data (1–3 h) and estimated the permeability by correcting the



**Fig. 7.** The logarithmic unilateral pressure difference when pressure is kept constant on one side. (a)  $V_{uD} = 0$ : Upstream pressure is maintained constant with different leakage rates; (b)  $V_{uD} = 0$ : Upstream pressure is maintained constant with different volume ratios; (c)  $V_{dD} = 0$ : Downstream pressure is maintained constant with different leakage rates; (d)  $V_{dD} = 0$ : Downstream pressure is maintained constant with different volume ratios.



**Fig. 8.** Experimental measurement results from Heller et al. (a) The upstream and downstream pressure. It is an unequal equilibrium. (b) Logarithms of the bilateral pressure difference and the unilateral downstream pressure difference. The bilateral pressure difference deviates from a straight line, and the unilateral pressure difference conforms to a straight line. The relative error between the permeability calculated from the proposed method and the one without correction exceeds 30 %.

assumed leak rate, ranging between 9.4–11.7 nD. The calculation result of the processing method proposed in this study is consistent with the original author’s estimates, and is supported by reasonable explanations and physical principles. If a gas leakage is overlooked and the late-time data is directly fitted with the logarithm of the bilateral pressure difference, the calculated permeability will yield a relative error exceeding 30 % compared to the true value.

#### 4. Conclusions

In permeability measurements of low-permeability porous media

such as unconventional natural gas reservoir rocks, gas leakage can significantly influence the results. This study models and solves the pulse-decay process under leakage conditions, subsequently developing related data processing and correction methods.

It was determined that when leakage is present, a stable trend of pressure decline and spatial pressure gradient occurs within the system, thus yielding a curve rather than a straight line when taking the logarithm of the bilateral pressure difference in the late-time stage. The concavity of this curve is associated with the leakage flow rate and the chamber size at both ends. Ignoring the impact of leakage and directly fitting the slope of the curve for permeability calculation can lead to

significant errors.

Through theoretical analysis, it was established that in the presence of leakage, the unilateral pressure difference over a given time interval can be utilized in the straight-line method for permeability calculation. The method corrects the permeability by eliminating the redundant term due to leakage in the analytical solution and is validated by experimental data from the literature. This provides a robust data processing method for permeability measurement by pulse decay method regardless of whether or not there is a leakage.

#### CRedit authorship contribution statement

**Mingbao Zhang:** Writing – original draft, Validation, Investigation. **Yue Wang:** Writing – original draft, Validation, Investigation. **Zhiguo Tian:** Writing – review & editing, Resources, Data curation. **Moran Wang:** Writing – review & editing, Supervision, Conceptualization.

#### Appendix

When the initial pressure difference is small enough, the boundary value problem of the pulse-decay process with gas leakage is constituted by Eqs. (7)–(10). The solution process is given in this appendix. Due to the presence of non-homogeneous terms in boundary conditions (8) and (9), the solution can be decomposed into two parts: the first part corresponds to the non-homogeneous boundary conditions, while the second part corresponds to the homogeneous boundary conditions:

$$P_D = P_1 + P_2. \quad (A1)$$

When  $P_1$  is being solved, the following assumption can be made:

$$\frac{\partial P_1}{\partial t_D} = \frac{\partial^2 P_1}{\partial x_D^2} = M. \quad (A2)$$

Hence,  $P_1$  can be written as follows:

$$P_1(x_D, t_D) = Mt_D + \frac{M}{2}x_D^2 + Nx_D. \quad (A3)$$

By substituting Eq. (A3) into the non-homogeneous boundary conditions, the expressions for  $M$  and  $N$  can be obtained (see Eq. (14)).

When solving for  $P_2$ , only the homogeneous boundary conditions need to be considered, that is, the leakage issue does not need to be considered. The impact of  $P_1$  on  $P_2$  is only reflected in the initial conditions:

$$P_2(x_D, 0) = \begin{cases} 1, & x_D = 0 \\ -\frac{M}{2}x_D^2 - Nx_D, & 0 < x_D \leq 1 \end{cases} \quad (A4)$$

Based on the separation of variables method [72], the expression for  $P_2$  can be obtained from the governing equation and homogeneous boundary conditions:

$$P_2(x_D, t_D) = C_0 + \sum_{m=1}^{\infty} C_m X_m(x_D) \exp(-\theta_m^2 t_D), \quad (A5)$$

where  $X_m$  represents the eigenfunction:

$$X_m = \theta_m \sin(\theta_m x_D) - V_{uD} \cos(\theta_m x_D), \quad m \geq 1. \quad (A6)$$

Here,  $\theta_m$  is the  $m$ th positive root of Eq. (13). For any functions  $P$  and  $Q$  defined over the interval  $[0, 1]$ , we define the inner product as:

$$\langle P, Q \rangle = V_{uD} V_{uD} \int_0^1 P(x)Q(x)dx + V_{uD}P(1)Q(1) + V_{uD}P(0)Q(0). \quad (A7)$$

$C_m$  represents the coefficient obtained from the orthogonal expansion of the initial condition of  $P_2$  with the eigenfunction set  $X_m$  as the basis:

$$C_m = \frac{\langle P_2(x_D, 0), X_m \rangle}{\langle X_m, X_m \rangle}, \quad m \geq 0. \quad (A8)$$

Finally, by superimposing Eq. (A5) and Eq. (A3), the comprehensive expression for  $P$  is obtained, as demonstrated in Eq. (12).

#### Declaration of competing interest

The authors declare that they have no known competing financial interests or personal relationships that could have appeared to influence the work reported in this paper.

#### Data availability

No data was used for the research described in the article.

#### Acknowledgements

This work was financially supported by NSFC of China grants (No. U1837602, 11761131012).

## References

- [1] Mukherjee M, Vishal V. Gas transport in shale: a critical review of experimental studies on shale permeability at a mesoscopic scale. *Earth-Sci Rev* 2023;244:104522.
- [2] Feng R, Chen S, Bryant S, Liu J. Stress-dependent permeability measurement techniques for unconventional gas reservoirs: review, evaluation, and application. *Fuel* 2019;256.
- [3] Huppert HE, Neufeld JA. The fluid mechanics of carbon dioxide sequestration. *Annu Rev Fluid Mech* 2014;46:255–72.
- [4] Boot-Handford ME, Abanades JC, Anthony EJ, Blunt MJ, Brandani S, Dowell NMac, Fernández JR, Ferrari M-C, Gross R, Hallett JP, Haszeldine RS, Heptonstall P, Lyngfelt A, Makuch Z, Mangano E, Porter RTJ, Pourkashanian M, Rochelle GT, Shah N, Yao JG, Fennell PS. Carbon capture and storage update. *Energy Environ Sci* 2014;7:130–89.
- [5] Song J, Zhang D. Comprehensive review of caprock-sealing mechanisms for geologic carbon sequestration. *Environ Sci Technol* 2013;47:9–22.
- [6] Birkholzer J, Houseworth J, Tsang C-F. Geologic disposal of high-level radioactive waste: status, key issues, and trends. *Annu Rev Env Resour* 2012;37:79–106.
- [7] Neuzil CE. Permeability of clays and shales. *Annu Rev Earth Pl Sc* 2019;47:247–73.
- [8] Liu ZB, Shao JF, Liu TG, Xie SY, Conil N. Gas permeability evolution mechanism during creep of a low permeable claystone. *Appl Clay Sci* 2016;129:47–53.
- [9] Sathyan K, Hsu HY, Lee SH, Gopinath K. Long-term lubrication of momentum wheels used in spacecrafts—An overview. *Tribol Int* 2010;43:259–67.
- [10] Joseph DD, Tao LN. Lubrication of a porous bearing—Stokes' solution. *Int J Appl Mech* 1966;33:753–60.
- [11] Lin JR, Hwang C-C. Hydrodynamic lubrication of finite porous journal bearings—Use of the brinkman-extended darcy model. *Int J Mech Sci* 1994;36:631–44.
- [12] Walder J, Nur A. Permeability measurement by the pulse-decay method: effects of poroelastic phenomena and non-linear pore pressure diffusion. *Int J Rock Mech Min* 1986;23:225–32.
- [13] Tian Z, Zhang D, Zhou G, Zhang S, Wang M. Compaction and sintering effects on scaling law of permeability-porosity relation of powder materials. *Int J Mech Sci* 2023;256.
- [14] Kang J, Wang M. Brinkman double-layer model for flow at a free-porous interface. *Int J Mech Sci* 2023.
- [15] Du S, Shi Y. Nanostructures in tight oil reservoirs: multiple perspectives. *Int J Hydrogen Energy* 2024;49:884–96.
- [16] Clarkson CR, Freeman M, He L, Agamalian M, Melnichenko YB, Mastalerz M, Bustin RM, Radliński AP, Blach TP. Characterization of tight gas reservoir pore structure using usans/sans and gas adsorption analysis. *Fuel* 2012;95:371–85.
- [17] Jones SC. A technique for faster pulse-decay permeability measurements in tight rocks. *SPE Form* 1997;12:19–25.
- [18] Ling K, He J, Pei P, Han G, Zhang H. Determining the permeability of tight rock with gas transient flow. *J Nat Gas Sci Eng* 2013;15:1–7.
- [19] Wang Z, Fink R, Wang Y, Amann-Hildenbrand A, Krooss BM, Wang M. Gas permeability calculation of tight rocks based on laboratory measurements with non-ideal gas slippage and poroelastic effects considered. *Int J Rock Mech Min* 2018;112:16–24.
- [20] Yousefi M, Dehghanpour H. A model and measurement technique for liquid permeability of tight porous media based on the steady-state method. *Energy Fuel* 2022;36:6860–7.
- [21] Gensterblum Y, Ghanizadeh A, Cuss RJ, Amann-Hildenbrand A, Krooss BM, Clarkson CR, Harrington JF, Zoback MD. Gas transport and storage capacity in shale gas reservoirs – a review. Part a: transport processes. *J Unconv Oil Gas Resour* 2015;12:87–122.
- [22] Wang Y, Liu S, Elsworth D. Laboratory investigations of gas flow behaviors in tight anthracite and evaluation of different pulse-decay methods on permeability estimation. *Int J Coal Geol* 2015;149:118–28.
- [23] Brace WF, Walsh JB, Frangos WT. Permeability of granite under high pressure. *J Geophys Res* 1968;73:2225–36.
- [24] Luffel DL, Guidry FK. New core analysis methods for measuring reservoir rock properties of devonian shale. *J Petrol Technol* 1992;44:11.
- [25] Jia B, Jin L, Smith SA, Bosshart NW. Extension of the gas research institute (gri) method to measure the permeability of tight rocks. *J Nat Gas Sci Eng* 2021;91.
- [26] Kranz RL, Saltzman JS, Blacic JD. Hydraulic diffusivity measurements on laboratory rock samples using an oscillating pore pressure method. *Int J Rock Mech Min* 1990;27:345–52.
- [27] Bernabé Y, Mok U, Evans B. A note on the oscillating flow method for measuring rock permeability. *Int J Rock Mech Min* 2006;43:311–6.
- [28] Lyu Q, Shi J, Gamage R, Pathegama. Effects of testing method, lithology and fluid-rock interactions on shale permeability: a review of laboratory measurements. *J Nat Gas Sci Eng* 2020;78:103302.
- [29] Metwally YM, Sondergeld CH. Measuring low permeabilities of gas-sands and shales using a pressure transmission technique. *Int J Rock Mech Min* 2011;48:1135–44.
- [30] Wang C, Pan L, Zhao Y, Zhang Y, Shen W. Analysis of the pressure-pulse propagation in rock: a new approach to simultaneously determine permeability, porosity, and adsorption capacity. *Rock Mech Rock Eng* 2019;52:4301–17.
- [31] Chenevert ME, Sharma AK. Permeability and effective pore pressure of shales. *SPE Drill Completion* 1993;8:28–34.
- [32] Alnoaimi KR, Kovscek AR. Influence of microcracks on flow and storage capacities of gas shales at core scale. *Transport Porous Med* 2019;127:53–84.
- [33] Nolte S, Fink R, Krooss BM, Amann-Hildenbrand A, Wang Y, Wang M, Schmatz J, Klaver J, Littke R. Experimental investigation of gas dynamic effects using nanoporous synthetic materials as tight rock analogues. *Transport Porous Med* 2021;137:519–53.
- [34] Rushing JA, Newsham KE, Lasswell PM, Cox JC, Blasingame TA. Klinkenberg-corrected permeability measurements in tight gas sands: steady-state versus unsteady-state techniques. In: *SPE Annual Technical Conference and Exhibition*; 2004.
- [35] Abdelmalek B, Karpyn ZT, Liu S, Yoon H, Dewers T. Gas permeability measurements from pressure pulse decay laboratory data using pseudo-pressure and pseudo-time transformations. *J Pet Explor Prod Te* 2017;8:839–47.
- [36] Jiang K, Zhou W, Tang C, Zhou Q, Xu H, Liu R, Zhao X. Pulse-decay permeability measurements and influencing factor analysis in marine shale formation in south china. *Arab J Geosci* 2021;14.
- [37] Hsieh PA, Tracy JV, Neuzil CE, Bredehoeft JD, Silliman SE. A transient laboratory method for determining the hydraulic properties of 'tight' rocks—I. Theory. *Int J Rock Mech Min* 1981;18:245–52.
- [38] Dicker AI, Smits RM. A practical approach for determining permeability from laboratory pressure-pulse decay measurements. *International Meeting on Petroleum Engineering* 1988.
- [39] Pan Z, Connell LD. Modelling permeability for coal reservoirs: a review of analytical models and testing data. *Int J Coal Geol* 2012;92:1–44.
- [40] Wang Y, Tian Z, Nolte S, Krooss BM, Wang M. An improved straight-line method for permeability and porosity determination for tight reservoirs using pulse-decay measurements. *J Nat Gas Sci Eng* 2022;105:104708.
- [41] Tian Z, Zhang D, Wang Y, Zhou G, Zhang S, Wang M. Inertial solution for high-pressure-difference pulse-decay measurement through microporous media. *J Fluid Mech* 2023;971:R1.
- [42] Wang Y, Tian Z, Nolte S, Krooss BM, Wang M. Influence of equation nonlinearity on pulse-decay permeability measurements of tight porous media. *Transport Porous Med* 2023;148:291–315.
- [43] Zhao Y, Zhang K, Wang C, Bi J. A large pressure pulse decay method to simultaneously measure permeability and compressibility of tight rocks. *J Nat Gas Sci Eng* 2022;98.
- [44] Yucel Akkutlu I, Fathi E. Multiscale gas transport in shales with local kerogen heterogeneities. *SPE J* 2012;17:1002–11.
- [45] Wang Y, Nolte S, Tian Z, Amann-Hildenbrand A, Krooss B, Wang M. A modified pulse-decay approach to simultaneously measure permeability and porosity of tight rocks. *Energy Sci Eng* 2021;9:2354–63.
- [46] Bourbie T, Walls J. Pulse decay permeability: analytical solution and experimental test. *SPE J* 1982;22:719–21.
- [47] Jones SC. A rapid accurate unsteady-state klinkenberg permeameter. *SPE J* 1972;12:383–97.
- [48] Shabani M, Krooss BM, Hallenberger M, Amann-Hildenbrand A, Fink R, Littke R. Petrophysical characterization of low-permeable carbonaceous rocks: comparison of different experimental methods. *Mar Petrol Geol* 2020;122:104658.
- [49] Jin G, Pérez HG, Al Dhamen AA, Ali SS, Nair A, Agrawal G, Khodja MR, Hussaini SR, Jangda ZZ, Ali AZ. Permeability measurement of organic-rich shale - comparison of various unsteady-state methods. In: *SPE Annual Technical Conference and Exhibition*; 2015.
- [50] Cui X, Bustin RM, Brezovski R, Nassichuk B, Glover K, Pathi V. A new method to simultaneously measure in-situ permeability and porosity under reservoir conditions: implications for characterization of unconventional gas reservoirs. *Canadian Unconventional Resources and International Petroleum Conference* 2010.
- [51] Yang Z, Sang Q, Dong M, Zhang S, Li Y, Gong H. A modified pressure-pulse decay method for determining permeabilities of tight reservoir cores. *J Nat Gas Sci Eng* 2015;27:236–46.
- [52] Yang S, Zhou HW, Zhang SQ, Ren WG. A fractional derivative perspective on transient pulse test for determining the permeability of rocks. *Int J Rock Mech Min* 2019;113:92–8.
- [53] Li Z, Ripepi N, Chen C. Using pressure pulse decay experiments and a novel multi-physics shale transport model to study the role of klinkenberg effect and effective stress on the apparent permeability of shales. *J Petrol Sci Eng* 2020:189.
- [54] Liu H-H, Lai B, Chen J, Georgi D. Pressure pulse-decay tests in a dual-continuum medium: late-time behavior. *J Petrol Sci Eng* 2016;147:292–301.
- [55] Sander R, Pan Z, Connell LD. Laboratory measurement of low permeability unconventional gas reservoir rocks: a review of experimental methods. *J Nat Gas Sci Eng* 2017;37:248–79.
- [56] Ghanizadeh A, Bhowmik S, Haeri-Ardakani O, Sanei H, Clarkson CR. A comparison of shale permeability coefficients derived using multiple non-steady-state measurement techniques: examples from the duvernay formation, alberta (canada). *Fuel* 2015;140:371–87.
- [57] Yang Z, Dong M, Zhang S, Gong H, Li Y, Long F. A method for determining transverse permeability of tight reservoir cores by radial pressure pulse decay measurement. *J Geophys Res-Sol Ea* 2016;121:7054–70.
- [58] Schmitt M, Fernandes CP, Wolf FG, Bellini da Cunha JA, Neto CP, Rahner VS, Santiago dos Santos. Characterization of brazilian tight gas sandstones relating permeability and angstrom-to micron-scale pore structures. *J Nat Gas Sci Eng* 2015;27:785–807.
- [59] Lu T, Xu R, Zhou B, Wang Y, Zhang F, Jiang P. Improved method for measuring the permeability of nanoporous material and its application to shale matrix with ultra-low permeability. *Materials* 2019:12.
- [60] Coria I, Martín I, Bouzid A-H, Heras I, Abasolo M. Efficient assembly of bolted joints under external loads using numerical fem. *Int J Mech Sci* 2018;142-143:575–82.

- [61] Glaser R. Multi-objective characterization of an inflatable space structure with a quasi-static experimental deflation and finite element analysis. *Int J Mech Sci* 2021;205.
- [62] Lasseux D, Jolly P, Jannot Y, Omnes ESB. Permeability measurement of graphite compression packings. *J Press Vessel Technol* 2011;133.
- [63] Song I, Rathbun AP, Saffer DM. Uncertainty analysis for the determination of permeability and specific storage from the pulse-transient technique. *Int J Rock Mech Min* 2013;64:105–11.
- [64] Boulin PF, Bretonnier P, Gland N, Lombard JM. Contribution of the steady state method to water permeability measurement in very low permeability porous media. *Oil Gas Sci Technol* 2012;67:387–401.
- [65] Heller R, Vermylen J, Zoback M. Experimental investigation of matrix permeability of gas shales. *AAPG Bull* 2014;98:975–95.
- [66] Liang Y, Price JD, Wark DA, Watson EB. Nonlinear pressure diffusion in a porous medium: approximate solutions with applications to permeability measurements using transient pulse decay method. *J Geophys Res-Sol Ea* 2001;106:529–35.
- [67] Liu M-M, Chen Y-F, Wei K, Zhou C-B. Interpretation of gas transient pulse tests on low-porosity rocks. *Geophys J Int* 2017;210:1845–57.
- [68] Wang X, Tan Y, Zhang T, Zhang J, Yu K. Diffusion process simulation and ventilation strategy for small-hole natural gas leakage in utility tunnels. *Tunn Undergr Sp Tech* 2020;97:103276.
- [69] Bhandari AR, Flemings PB, Polito PJ, Cronin MB, Bryant SL. Anisotropy and stress dependence of permeability in the barnett shale. *Transport Porous Med* 2015;108:393–411.
- [70] Garg R, Agrawal A. Poiseuille number behavior in an adiabatically choked microchannel in the slip regime. *Phys Fluids* 2020;32.
- [71] Shan X, Wang M. On mechanisms of choked gas flows in microchannels. *Phys Lett A* 2015;379:2351–6.
- [72] Wang Y, Tian Z, Nolte S, Amann-Hildenbrand A, Krooss BM, Wang M. Reassessment of transient permeability measurement for tight rocks: the role of boundary and initial conditions. *J Nat Gas Sci Eng* 2021;95:104173.